Selective Aerobic Oxidation of Vanillyl Alcohol to Vanillin Catalysed by Nanostructured Ce-Zr-O Solid Solutions

P. R. G. Nallappa Reddy, Bolla Govinda Rao, Tumula Venkateshwar Rao & Benjaram M. Reddy

Catalysis Letters

ISSN 1011-372X
Volume 149
Number 2

Catal Lett (2019) 149:533-543
DOI 10.1007/s10562-019-02658-1

Springer

Catalysis Letters (2019) 149:533–543
https://doi.org/10.1007/s10562-019-02658-1

Selective Aerobic Oxidation of Vanillyl Alcohol to Vanillin Catalysed by Nanostructured Ce-Zr-O Solid Solutions

P. R. G. Nallappa Reddy[1,2] · Bolla Govinda Rao[1,2] · Tumula Venkateshwar Rao[1,2] · Benjaram M. Reddy[1,2]

Received: 6 November 2018 / Accepted: 7 January 2019 / Published online: 17 January 2019

Abstract

A series of Ce_{1-x}–$Zr_xO_{2-\delta}$ (x = 0.2, 0.5, and 0.8) mixed oxides were prepared by coprecipitation method and explored for selective oxidation of vanillyl alcohol employing O_2 and acetonitrile as the oxidant and solvent, respectively under base-free conditions. To ascertain the key factors responsible for vanillyl alcohol oxidation, the physicochemical properties of the synthesized catalysts were investigated by various characterization techniques namely, XRD, BET surface area, Raman, XPS, and H_2-TPR. It was observed from this exercise that the catalytic activity dependents on the Ce:Zr mole ratio, which is related to the degree of reducibility of the catalyst. Interestingly, the catalytic activity is enhanced with the increase of Ce content in the Ce–Zr mixed oxide. Among the investigated catalysts, the $Ce_{0.8}Zr_{0.2}O_2$ combination exhibited a high catalytic activity with ~98% conversion and ~99% selectivity to vanillin. Smaller crystallite size, large BET surface area, more number of oxygen vacancies, improved redox properties, and strong synergetic interaction are found to be the key factors to promote the oxidation ability of $Ce_{0.8}Zr_{0.2}O_2$ catalysts towards vanillyl alcohol oxidation. Further, the influence of reaction parameters such as time, solvent, temperature, and oxygen pressure were also studied to optimize the catalytic process for vanillyl alcohol oxidation. As revealed by these studies, the high activity of $Ce_{0.8}Zr_{0.2}O_2$ catalyst could be retained up to five cycles without appreciable loss in the activity and selectivity.

Graphical Abstract

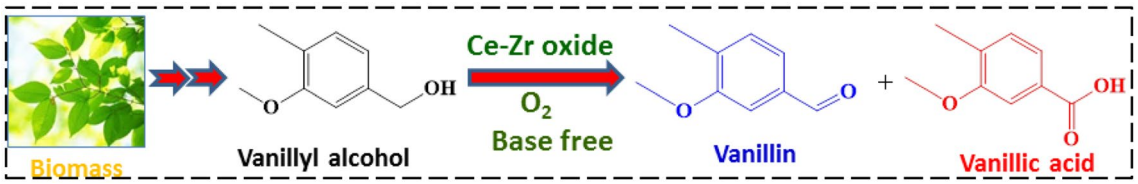

Nanosized $Ce_{0.8}Zr_{0.2}O_2$ catalyst exhibited an excellent catalytic activity and superior selectivity to vanillin in the liquid phase oxidation of vanillyl alcohol under ecofriendly conditions

Keywords Ceria · Vanillyl alcohol · Vanillin · Oxygen vacancy · Redox properties

1 Introduction

The effective utilization of renewable organic carbon feedstock as alternative to fossil fuels is crucial for long-term economic and social stability [1]. Among the various renewable resources, lignocellulosic biomass is recognized as a promising organic carbon feedstock for the sustainable production of fuels and chemicals, and it is the fourth largest source of energy in the world. Lignocellulose biomass is mainly composed of hemicellulose (23–32%), cellulose

Electronic Supplementary Material The online version of this article (https://doi.org/10.1007/s10562-019-02658-1) contains supplementary material, which is available to authorized users.

✉ Benjaram M. Reddy
bmreddy@iict.res.in; mreddyb@yahoo.com

[1] Catalysis and Fine Chemicals Department, CSIR—Indian Institute of Chemical Technology, Uppal Road, Hyderabad 500 007, India

[2] Academy of Scientific and Innovative Research, CSIR-IICT, Hyderabad, India

(38–50%), and lignin (15–25%) [2]. Due to the complexity of lignin moiety, the effective utilization of lignin could play a crucial role in the bio-refinery industry as it contains aromatic structure, from which a variety of aromatic chemicals and fuel grade chemicals could be obtained [3, 4]. A variety of state-of-art strategies have been developed for the production of value-added chemicals and fuel grade chemicals from lignin moiety. Among them, selective catalytic oxidation of lignin derived vanillyl alcohol has been paid immense research interest owing to the numerous applications of vanillin in food additives, perfumes, pharmaceuticals, and cosmetics [5]. Further, glyoxylic and nitrose methods were also reported as traditional routes to produce vanillin from guaiacol, however, these methods inherently suffer with serious drawbacks [6, 7].

To tackle the above shortcomings, development of green catalytic methodologies alternative to traditional approaches is highly needed by the scientific community. In this direction, considerable research efforts have been devoted for the construction of various homogeneous and heterogeneous catalytic systems to explore the oxidation of vanillyl alcohol [8, 9]. However, low yield of desired product, poor separation, and inefficient recyclability constrained the practical utilization of homogeneous catalysts [10, 11]. The feasible advantages such as simple handling, effective separation, and recyclability make heterogeneous catalysts as promising alternatives to explore the oxidation of vanillyl alcohol. Indeed supported noble metal catalysts such as Au/CeO_2, Pt/C, and Ru/TiO_2 were found to be active for oxidation of various alcohols. However, limited availability and high cost hindered their commercial application in the chemical industry [12–14]. As a consequence, transition metal oxides were exploited as viable alternatives to the noble metals due to versatile properties of metal oxides such as inexpensive nature, variable oxidation states, and excellent redox ability [6, 15].

Currently, significant efforts have been devoted to the development of metal oxides and mixed metal oxide catalysts for oxidation of vanillyl alcohol. In this regard, spinel Co-Mn mixed oxide was exploited as an efficient catalyst in the presence of a base (NaOH) [7]. On the other hand, Hamid et al. have developed $CuZrO_3$ catalyst that afforded ~91% conversion of vanillyl alcohol with moderate selectivity to vanillin (~76%) [16]. Jha et al. investigated a wide variety of oxide catalysts such as Co_3O_4, Co–Mn oxides, and Co–Mn supported on graphene, and reported to be active for vanillyl alcohol oxidation [6, 7, 15, 17]. However, some of these catalysts are inactive in the absence of base. Very recently, Reddy et al. investigated Mn doped CeO_2 and demonstrated that it is an efficient catalyst for oxidation of vanillyl alcohol in terms of conversion and vanillin selectivity [8]. In general, most of the catalysts reported so far for this reaction suffer from the vanillin selectivity [6, 18, 19]. Therefore, an extensive research work is essential to improve the catalytic efficiency and selectivity to vanillin by developing highly active and selective catalysts.

Owing to their unique redox properties, and high oxygen storage capacity, ceria-based (CeO_2) catalysts are playing a significant role in oxidation reactions [20, 21]. It has been reported that redox properties and defect sites (oxygen vacancies) together promote the oxidation of vanillyl alcohol [8]. Therefore, it is believed that by tuning the physicochemical features of CeO_2, its catalytic performance could be improved for vanillyl alcohol oxidation. The modification of CeO_2 properties could be accomplished by doping of transition or rare earth metal ions into the ceria lattice, thereby improved catalytic activity [22–25]. Recently, considerable research work has been carried out to develop Zr-doped CeO_2 mixed oxides because of their high oxygen storage capacity and better redox properties, which eventually contribute to the enhancement of catalytic activity for various reactions [26–30]. The present investigation was undertaken against the aforesaid background. The main aim of this work is to investigate the effect of Ce/Zr mole ratio on the physicochemical properties and the catalytic performance for liquid phase oxidation of vanillyl alcohol employing O_2 and acetonitrile as the oxidant and the solvent under base-free conditions, respectively. Accordingly, we have synthesized nanostructured CeO_2–ZrO_2 mixed oxides with different Ce/Zr mole ratios by adopting a facile preparation method. A systematic physicochemical characterisation of the developed catalysts has been achieved using X-ray diffraction (XRD), Brunauer-Emmet-Teller (BET) surface area, Raman spectroscopy, X-ray photoelectron spectroscopy (XPS), transmission electron microscopy (TEM), and H_2-temperature programmed desorption (H_2-TPR) techniques to correlate with their catalytic results. The influence of reaction parameters was also investigated to optimise the reaction conditions for efficient oxidation of vanillyl alcohol.

2 Experimental

2.1 Catalyst Preparation

A series of Ce_{1-x}–$Zr_xO_{2-\delta}$ (x = 0.2, 0.5, and 0.8) mixed oxides, namely, $Ce_{0.8}Zr_{0.2}O_2$, $Ce_{0.5}Zr_{0.5}O_2$, and $Ce_{0.2}Zr_{0.8}O_2$ were synthesized by a facile coprecipitation method using cerium(III) nitrate hexahydrate (Aldrich, AR grade) and zirconium(IV) oxynitrate hydrate (Aldrich, AR grade) as the metal precursors. The requisite amounts of metal precursors were dissolved separately in double distilled water under mild stirring conditions and mixed together. Dilute aqueous NH_3 solution (precipitating agent) was added drop-wise manner to the above solution under continuous stirring until it reaches pH ~9 at room temperature. Then the stirring of

mixture was continued for 24 h followed by 2 days of aging. The obtained precipitate was filtered off, washed thoroughly with distilled water until it was free from anion impurities, and dried at 393 K for 12 h. The obtained final cake was crushed in ceramic mortar in order to get the fine powder and the resultant powder was calcined at 773 K for 5 h at a heating rate of 5 K min^{-1} in air atmosphere. Similarly, we have adopted the above described procedure to prepare pure CeO_2 and ZrO_2 for comparison purpose.

2.2 Catalyst Characterization

Powder XRD patterns of the prepared samples were recorded on a Rigaku diffractometer using Cu Kα radiation (1.540 Å), operated at 40 kV and 40 mA. The diffractograms were recorded in the 2θ range of 10–80° with a 2θ step size of 0.02° and a step time of 2.4 s. The XRD phases present in the samples were identified with the help of Powder Diffraction File-International Centre for Diffraction Data (PDF-ICDD). The average crystallite size and lattice parameter of the prepared samples were calculated using the full width at half maximum (FWHM) of the (111) peak using the Debye–Scherer equation and the cubic indexation method respectively.

The Brunauer–Emmett–Teller (BET) surface areas of the samples were determined by N_2 adsorption on a Micromeritics Gemini 2360 instrument. Before the analysis, the samples were oven–dried at 393 K for 12 h and flushed with Argon gas for 2 h to remove any surface-adsorbed residue. Surface area was calculated by utilizing the desorption data. Raman spectra of the samples were recorded on a Horiba Jobin–Yvon HR800 Raman spectrometer equipped with a liquid-nitrogen cooled charge coupled device (CCD) detector and a confocal microscope. The emission line at 638 nm from Ar^+ laser (Spectra Physics) was focused on the sample under the microscope with the diameter of the analysed spot being ~ 1 μm, under ambient conditions. The time of acquisition was adjusted according to the intensity of Raman scattering. The wavenumber values obtained were precise to within 2 cm^{-1}.

The TEM-HREM studies were made on a TECNAIG2 TEM microscope equipped with a slow-scan CCD camera and at an accelerating voltage of 200 kV. The carbon coated Cu grid was used for the preparation of samples for TEM analysis. The preparation of samples for TEM-HREM analysis involved sonication in ethanol for 2–5 min followed by deposition of a drop on a copper grid. The specimen was examined under vacuum at room temperature. The XPS measurements were performed on a PHI 5400 instrument. Al Kα radiation (1486.6 eV) X-ray source was used for XPS analysis and at a pressure lower than 10^{-7} Torr. The sample preparation for XPS analysis involved mounting of a few grams of sample on a carbon tape supported with a silica plate. The resultant plate supported with a holder was placed in the vacuum chamber of Thermo K-Alpha XPS instrument before the start of analysis. Thermo-Avantage Software was used for XPS analysis of the prepared samples. The binding energies of Ce, Zr, and O were charge-corrected with respect to the adventitious carbon (C 1 s) peak at 284.6 eV. Flood gun was used to remove the static charge that developed on the sample surface during XPS analysis.

The reducibility of the synthesized samples was estimated by H_2-TPR analysis, using a thermal conductivity detector of a gas chromatograph (Schimadzu). Approximately 30 mg of the sample was loaded in an isothermal zone of the reactor and were treated in a helium gas flow at 400 K followed by cooling to room temperature. After that, flow of the He was switched to 5% H_2/Ar with a rate of 20 ml min^{-1} and the temperature was linearly increased to 1073 K at a heating ramp of 5 K min^{-1}, keeping all the parameters un-changed. The hydrogen consumption during the reduction process was estimated by passing the effluent gas through a molecular sieve trap to remove the produced water and was analysed by gas chromatography using a thermal conductivity detector.

2.3 Catalytic Activity Test

The liquid phase oxidation of vanillyl alcohol was carried out using O_2 as the oxidant and acetonitrile as the solvent. The reaction was performed in a 100 ml Parr stainless steel autoclave reactor. A mixture of vanillyl alcohol (3 mmol), acetonitrile (20 ml), and the catalyst (0.15 g) were charged into the reactor and the reaction temperature and pressure were maintained at 413 K and 20 bar oxygen pressure respectively. Then the reaction mixture in the reactor was agitated at 1000 rpm and the process was continued for desired time. After completion of the reaction, the reactor was cooled to room temperature, the unabsorbed gas in the reactor was vented out and the final volume was recorded. Then, the liquid products and the catalyst were separated by simple centrifugation. The obtained products were further diluted with acetonitrile solvent and analysed by GC equipped with a BP-20 (wax) capillary column and a flame ionization detector. The products were confirmed by GC–MS equipped with a DB-5 capillary column and mass detector. The reaction products were also confirmed by injecting the corresponding authentic compounds in the GC.

3 Results and Discussion

3.1 XRD Analysis

The XRD patterns of Ce_{1-x}–$Zr_xO_{2-\delta}$ (x = 0.2, 0.5, and 0.8) mixed oxides including pure CeO_2 calcined at 773 K are illustrated in Fig. 1. A close observation of

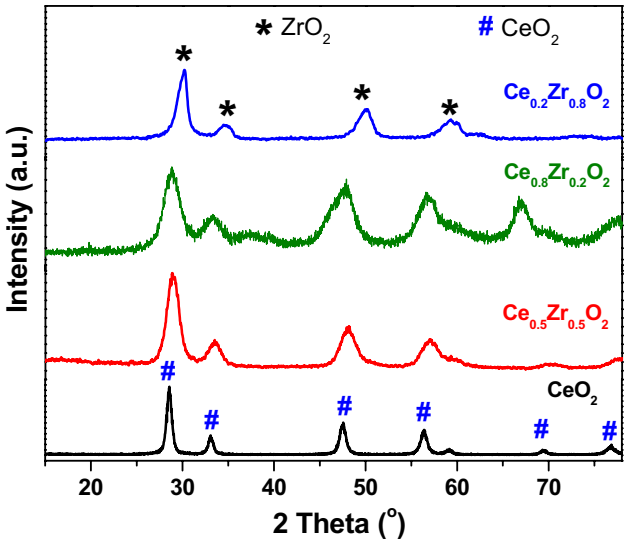

Fig. 1 Powder XRD profiles of pure CeO_2, $Ce_{0.5}Zr_{0.5}O_2$, $Ce_{0.8}Zr_{0.2}O_2$, and $Ce_{0.2}Zr_{0.8}O_2$ samples

Fig. 1 reveals that the XRD patterns of $Ce_{0.5}Zr_{0.5}O_2$ and $Ce_{0.8}Zr_{0.2}O_2$ samples could be readily indexed to (111), (200), (220), (311), (331), and (400) planes, which are characteristic of the fluorite like cubic structure of CeO_2 [31–33]. This scrutiny demonstrates that in-situ doping did not alter the cubic structure of pure CeO_2. Further, no evidence of the peaks related to ZrO_2 in the XRD profiles of $Ce_{0.5}Zr_{0.5}O_2$ and $Ce_{0.8}Zr_{0.2}O_2$ samples confirm the formation of Ce–Zr–O solid solutions. In contrast, a high amount of Zr doped Ce sample ($Ce_{0.2}Zr_{0.8}O_2$) shows XRD peaks corresponding to ZrO_2 with tetragonal phase [31]. Further, no XRD lines related to CeO_2 phase were identified for $Ce_{0.2}Zr_{0.8}O_2$ sample. A striking observation noticed from Fig. 1 is that cubic CeO_2 and t-ZrO_2 phases were dominated in the $Ce_{0.5}Zr_{0.5}O_2$, $Ce_{0.8}Zr_{0.2}O_2$ and $Ce_{0.2}Zr_{0.8}O_2$ samples, respectively. In addition, the diffraction patterns of $Ce_{0.5}Zr_{0.5}O_2$ and $Ce_{0.8}Zr_{0.2}O_2$ samples are quite broader and shifted to higher two-theta values in comparison to pure CeO_2. Lattice contraction (substitution of Ce^{4+} (~0.87 Å) by smaller sized Zr^{4+} (~0.72 Å) dopant cations) is expected to be a probable reason for peak shifting [34]. The average crystallite size and lattice parameter of all samples were determined with the help of Scherrer equation and the obtained values are presented in Table 1. The crystallite size of the doped Ce samples was found to decrease in comparing to pure CeO_2 (Table 1). This observation is due to the fact that the incorporation of dopant is expected to arrest the crystal growth of CeO_2 through the formation of Ce–Zr–O solid solutions. The average crystallite size was found to be 8.9, 6.0, and 5.6 nm for CeO_2, $Ce_{0.5}Zr_{0.5}O_2$, and $Ce_{0.8}Zr_{0.2}O_2$ samples, respectively.

Table 1 BET surface area (S), average crystallite size (D), lattice parameter (LP), Raman shift of CeO_2, $Ce_{0.5}Zr_{0.5}O_2$, $Ce_{0.8}Zr_{0.2}O_2$, and $Ce_{0.2}Zr_{0.8}O_2$ catalysts

Sample	S (m^2g^{-1})[a]	D (nm)[b]	LP (nm)[b]	Raman shift F_{2g} (cm^{-1})
CeO_2	38 ± 2	8.9 ± 1	0.540 ± 0.05	458
$Ce_{0.5}Zr_{0.5}O_2$	71.6 ± 2	6.0 ± 1	0.535 ± 0.05	464
$Ce_{0.8}Zr_{0.2}O_2$	137.1 ± 2	5.6 ± 1	0.529 ± 0.05	474
$Ce_{0.2}Zr_{0.8}O_2$	50.5 ± 2	–	–	–

3.2 BET Analysis

To determine the textural properties of as prepared CeO_2–ZrO_2 solid solutions, N_2-adsorption and desorption studies were undertaken and the obtained values are summarized in Table 1. It is well-known that mixed oxides exhibit larger BET surface areas than the individual single oxides, due to the cooperative effect of respective oxides in the final mixed oxides. As stated, surface area of CeO_2 was significantly improved after incorporation of dopant metal ions. The existence of strong synergetic interaction between the dopant metal oxide and the host metal oxide enables to arrest the crystal growth of CeO_2 thereby decreases its crystallite size and enhances its surface area to some extent. Interestingly, surface area of doped CeO_2 was found to enhance with the increase of Ce content. The specific surface area of CeO_2, $Ce_{0.5}Zr_{0.5}O_2$, $Ce_{0.8}Zr_{0.2}O_2$ and $Ce_{0.2}Zr_{0.8}O_2$ samples were found to be ~38, ~71.6, ~137.1 and ~50.5 m^2/g, respectively, which corroborate well with the crystallite size decrease (Table 1).

3.3 Raman Analysis

It is well-known that Raman spectroscopy is a sensitive probe to estimate the defect sites present in the CeO_2 based samples. Figure 2 represents the Raman spectra of $Ce_{0.5}Zr_{0.5}O_2$, $Ce_{0.8}Zr_{0.2}O_2$, $Ce_{0.2}Zr_{0.8}O_2$, and undoped CeO_2 samples calcined at 773 K. The appearance of high intense sharp band at ~465 cm^{-1} is attributed to F_{2g} Raman active mode of fluorite structure CeO_2 for $Ce_{0.5}Zr_{0.5}O_2$ and $Ce_{0.8}Zr_{0.2}O_2$ samples (supported by XRD results) [35, 36]. On the other hand, the observed disappearance of Raman bands related to ZrO_2 phase for $Ce_{0.5}Zr_{0.5}O_2$ and $Ce_{0.8}Zr_{0.2}O_2$ samples indicate the formation of Ce–Zr–O solid solutions as evidenced by XRD analysis. It is noticed from Fig. 2 that the F_{2g} band for doped CeO_2 ($Ce_{0.5}Zr_{0.5}O_2$ and $Ce_{0.8}Zr_{0.2}O_2$) sample is quite different from pure CeO_2 in terms of broadening and peak shifting. The shift in F_{2g} mode is due to the change in the M–O vibration frequency after Zr^{4+} incorporation into the CeO_2 lattice, which account for the difference in the ionic radius of Ce^{4+} (~0.87 Å) and Zr^{4+} (~0.72 Å)

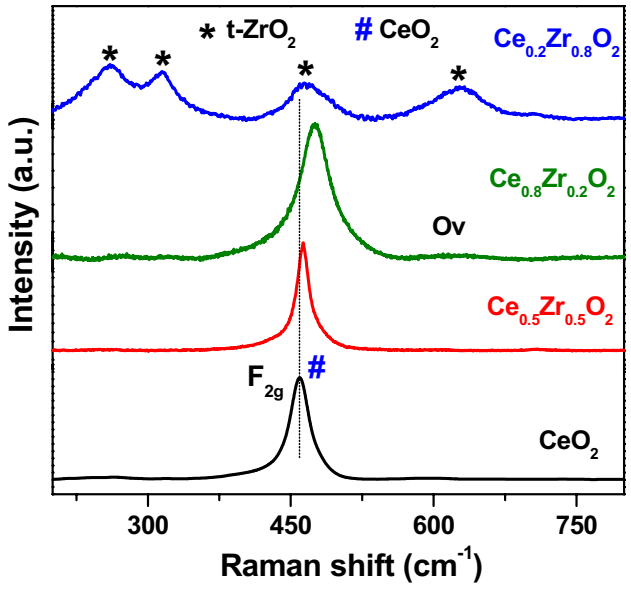

Fig. 2 Raman spectra of pure CeO_2, $Ce_{0.5}Zr_{0.5}O_2$, $Ce_{0.8}Zr_{0.2}O_2$, and $Ce_{0.2}Zr_{0.8}O_2$samples

ions. Further, F_{2g} peak shift and its broadening are more pronounced in the case of $Ce_{0.8}Zr_{0.2}O_2$ sample. Interestingly, we observed a low intensity peak at ~620 cm^{-1} only for $Ce_{0.8}Zr_{0.2}O_2$ sample which signifies the presence of oxygen vacancies, which are expected to play a key role in the oxidation catalysis [37]. Thus, we expected a high catalytic performance for this catalyst for the oxidation of vanillyl alcohol. It can be noted from the figure that the Ce/Zr mole ratio plays a significant role in the creation of oxygen vacancies in Ce–Zr–O solid solutions. In contrast, the high Zr doped CeO_2 sample i.e., $Ce_{0.2}Zr_{0.8}O_2$ shows Raman bands at around ~260, ~316, and ~630 cm^{-1}, which are typically assigned to the tetragonal ZrO_2 (t-ZrO_2). In addition, we noticed a strong band at ~467 cm^{-1} attributed to the Raman active mode of c-phase of ZrO_2 [31]. It is clearly observed from Raman results that cubic CeO_2 phase is dominated in the $Ce_{0.5}Zr_{0.5}O_2$ and $Ce_{0.8}Zr_{0.2}O_2$ catalysts, respectively. On the other hand, t-ZrO_2 phase is prominent in the $Ce_{0.2}Zr_{0.8}$ in accordance with XRD results.

3.4 TEM Studies

In order to know the morphology and particle size distribution, we have undertaken TEM studies over the identified high efficient $Ce_{0.8}Zr_{0.2}O_2$ catalyst. Figure 3 represents the TEM and HREM images of $Ce_{0.8}Zr_{0.2}O_2$ sample calcined at 773 K. As can be noted from the figure, spherical shaped particles with uniform distribution are found for $Ce_{0.8}Zr_{0.2}O_2$ sample.The estimated particle size is found to be in the range of ~6–7 nm in accordance with the crystallite size obtained from XRD results. Figure 3b shows a lattice d-spacing of ~0.31 nm corresponding to the distance between the adjacent (111) crystal planes of the fluorite-structured CeO_2 [38].

3.5 XPS Analysis

XPS analysis was performed to elucidate the information regarding the chemical states of the elements present on the surface of the samples. Figure 4 depicts the deconvoluted Ce 3d core level spectra for all Ce–Zr–O solid solutions along with pure CeO_2. It is obvious that Ce 3d core level spectra of all samples exhibit eight peaks, which are classified into two spin orbit multiplets namely, Ce $3d_{3/2}$ and Ce $3d_{5/2}$ contributions. The peaks denoted by u are due to $3d_{3/2}$ spin orbit state, whereas the peaks corresponds to v are due to $3d_{5/2}$ spin orbit state. As can be seen from the Fig. 4, the peaks categorized by v, v'', v''', u, u'', and u''' indicate the $3d^{10}4f^0$ electronic state of Ce^{4+}, while the peaks labelled by u' and v' signify the Ce^{3+} with the electronic configuration of $3d^{10}4f^1$ [39, 40]. Thus, it can be concluded that all catalysts contain Ce^{4+} as well as Ce^{3+} ions, indicating the redox nature of the synthesized catalysts [41]. Interestingly, irrespective of Ce/Zr mole

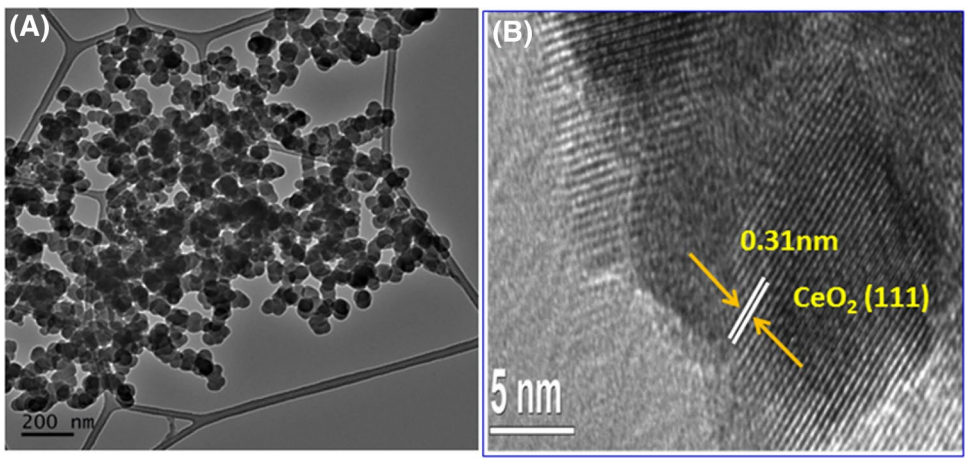

Fig. 3 **a** TEM and **b** HRTEM images of $Ce_{0.8}Zr_{0.2}O_2$ catalyst

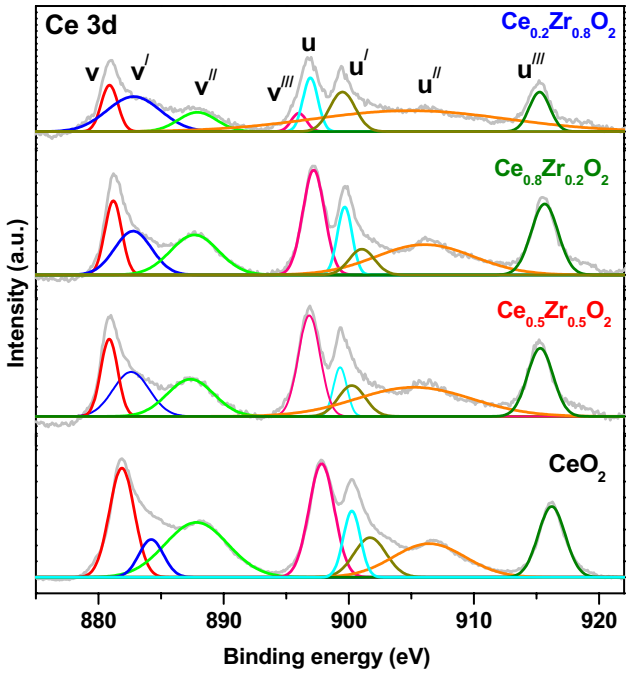

Fig. 4 Ce 3d XP spectra of pure CeO_2, $Ce_{0.5}Zr_{0.5}O_2$, $Ce_{0.8}Zr_{0.2}O_2$, and $Ce_{0.2}Zr_{0.8}O_2$ samples

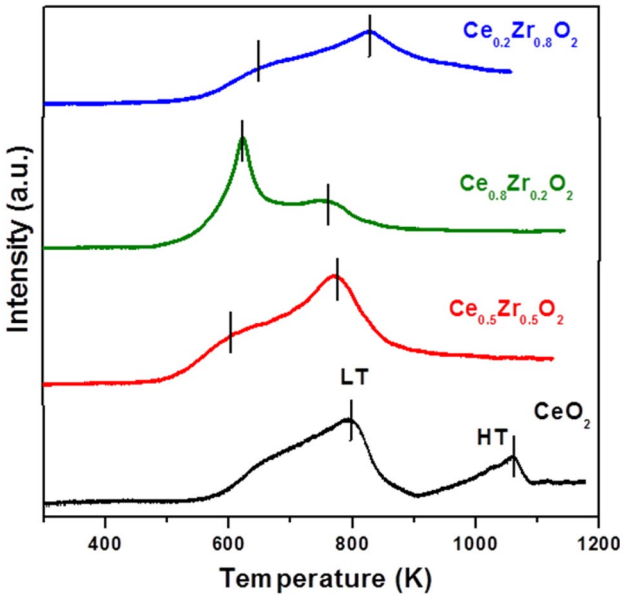

Fig. 5 H_2-TPR profiles of pure CeO_2, $Ce_{0.5}Zr_{0.5}O_2$, $Ce_{0.8}Zr_{0.2}O_2$, and $Ce_{0.2}Zr_{0.8}O_2$ samples

ratio, the electronic binding energies of the Ce–Zr–O solid solutions were found to shift towards lower binding energy side compared to that of pure CeO_2. Modification of the Ce–O environment by the dopant ions is one of the valid reasons for the observed shift in the binding energy [42].

Figure S1 shows the deconvoluted O 1 s spectra of all Ce–Zr–O solid solutions. It is obvious from the figure that, various kinds of oxygen species were noticed for all samples. For CeO_2, we observed a peak at lower binding energy (~ 529.2 eV) which is related to CeO_2 lattice oxygen. Another peak situated at ~ 531.5 eV is attributed to the adsorbed oxygen species of hydroxyl groups. Finally, the peak observed at high binding energy side (~ 533.3 eV) is ascribed to adsorbed molecular water and carbonate species [42, 43]. In addition, we found a notable variation in the binding energies of all Ce–Zr–O solid solutions compared to pure CeO_2. Fig. S2 shows the Zr 3d XP spectra of $Ce_{0.5}Zr_{0.5}O_2$, $Ce_{0.8}Zr_{0.2}O_2$, and $Ce_{0.2}Zr_{0.8}O_2$ catalysts. Irrespective of the sample, we observed two bands at around 180.7–181.65 eV ($3d_{3/2}$) and 183.0–183.5 eV ($3d_{5/2}$), indicating the presence of Zr^{+4} ions in the synthesized catalysts [27].

3.6 H_2-TPR Studies

It is a well established fact that the redox property of catalyst has a direct influence on its catalytic performance for many catalytic reactions. Therefore, we have carried out TPR analysis on various samples synthesized in this study. The H_2-TPR profiles of Ce–Zr–O solid solutions with different Ce/Zr ratios are shown in Fig. 5. As can be noticed from the figure, irrespective of Ce/Zr mole ratio, two reduction peaks were observed for Ce–Zr–O solid solutions in line with the undoped CeO_2. It is obvious from the Fig. 5 that the pure CeO_2 exhibits two reduction peaks, in which first peak is situated at low temperature (793 K), due to the surface reduction (outermost layers of Ce^{+3}) of CeO_2, whereas the appearance of another peak at high temperature region (1060 K) is attributed to the bulk reduction of (inner layers of Ce^{+3}) CeO_2 [44]. However, both the reduction profiles of $Ce_{0.5}Zr_{0.5}O_2$ and $Ce_{0.8}Zr_{0.2}O_2$ samples are notably shifted to lower temperature compared to that of pure CeO_2 indicating that dopant significantly modifies the redox properties of CeO_2. For example, $Ce_{0.5}Zr_{0.5}O_2$ shows two reduction peaks at 633 and 775 K for surface and bulk reductions respectively. In the case of $Ce_{0.8}Zr_{0.2}O_2$ sample, we observed a huge decrease in the surface (620 K) and bulk (758 K) reduction temperatures compared to that of $Ce_{0.5}Zr_{0.5}O_2$ and CeO_2 samples. This interesting observation reveals that the Ce/Zr mole ratio shows a remarkable influence on the reduction temperature of the sample. Moreover, the redox property of the catalyst is generally associated with the formation of oxygen vacancies, which are likely to play a key role in promoting the oxidation reactions. Therefore, we can expect more oxygen vacancies over $Ce_{0.8}Zr_{0.2}O_2$ sample because of high redox ability which may result in higher catalytic activity for vanillyl alcohol oxidation. To our surprise, the high Zr contacting Ce solid solution ($Ce_{0.2}Zr_{0.8}O_2$) showed

two reduction peaks relatively at high temperatures (656 and 830 K) than that of Ce enriched samples ($Ce_{0.5}Zr_{0.5}O_2$ and $Ce_{0.8}Zr_{0.2}O_2$), which could be attributed to the irreducible nature of ZrO_2 [45].

3.7 Screening of Catalysts

Oxidation of lignin moiety was investigated by choosing vanillyl alcohol as a model lignin compound. Typically the catalytic oxidation of vanillyl alcohol delivers vanillin and vanillic acid as the products. Firstly, we have performed the oxidation of vanillyl alcohol under the absence of catalyst, which reveals poor activity (~15%) (Table 2, entry 1). This result clearly indicates the key role of catalyst to promote the oxidation reaction. Further, optimization of the reaction conditions is one of the critical aspects in heterogeneous catalysis. In this regard, we have performed the oxidation of vanillyl alcohol at 413 K, 20 bar O_2 pressure, and acetonitrile as the solvent for 5 h using CeO_2 and ZrO_2 catalysts, which showed ~40% and ~30% conversions, respectively (Table 2, entries 2 and 3). Moreover, both the catalysts show a high selectivity (~96–98%) to vanillin product. To our delight, ~28 and ~20% of conversions were obtained over the commercial CeO_2 and ZrO_2 catalysts, respectively (Table 2, entries 4 and 5). This interesting result indicates that synthesized catalysts are more promising than the commercial samples. To envisage the role of Ce/Zr mole ratio towards the oxidation of vanillyl alcohol, Ce–Zr mixed oxides with different Ce/Zr mole ratios were tested under the identical reaction conditions and the obtained results are summarized in Table 2. As can be noted from Table 2, the Ce/Zr mole ratio shows a remarkable influence on the catalytic activity of Ce–Zr mixed oxides. For example, $Ce_{0.5}Zr_{0.5}O_2$ catalyst provided ~75% conversion with ~97.1% selectivity to vanillin (Table 2, entry 6). In parallel, the conversion of vanillyl alcohol was found to increase from ~75 to ~98% with the increase of Ce/Zr mole ratio (Table 2, entry 7). Surprisingly, when the Zr concentration increases a remarkable drop in the conversion from ~98 to ~58% was attained for $Ce_{0.2}Zr_{0.8}O_2$ catalyst, and it shows a high selectivity (~96.9%) to vanillin indicating that CeO_2 species are more efficient than ZrO_2 species (Table 2, entry 8). Performance of the oxidation of vanillyl alcohol under the absence of air resulted in poor conversion indicating the necessity of oxidant to accelerate the rate of reaction (Table 2, entry 9). Further, a low activity (~55%) was obtained with physical mixtures of CeO_2 and ZrO_2 at 413 K, 20 bar O_2 pressure, and acetonitrile solvent for 5 h (Table 2, entry 10). It confirms the crucial role of synergetic interaction to promote the oxidation reaction. In order to know the significance of $Ce_{0.8}Zr_{0.2}O_2$ catalyst, various reaction parameters such as temperature, pressure, solvent, and the reaction time were investigated and the obtained results are discussed in the following paragraphs.

Table 2 Selective oxidation of vanillyl alcohol over Ce–Zr mixed oxides with different Ce/Zr mole ratios

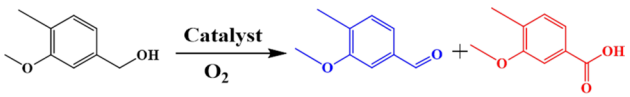

Vanillyl alcohol Vanillin Vanillic acid

Entry	Catalyst	Conv. of vanillyl alcohol	Sel. to vanillin
1	Blank	15	–
2	CeO_2	40	97.2
3	ZrO_2	30	96.8
4	Commercial CeO_2	28	94.5
5	Commercial ZrO_2	20	93.8
6	$Ce_{0.5}Zr_{0.5}O_2$	75	97.1
7	$Ce_{0.8}Zr_{0.2}O_2$	98	99.0
8	$Ce_{0.2}Zr_{0.8}O_2$	58	96.9
9[b]	$Ce_{0.8}Zr_{0.2}O_2$	26	97.6
10[c]	$CeO_2 + ZrO_2$	55	96.6

Reaction conditions: vanillyl alcohol (3 mmol), catalyst (150 mg), O_2 pressure (20 bar), time (5 h), and temperature (413 K)

[b]Without O_2

[c]Physical mixture

3.8 Effect of Solvent

It is generally accepted that nature of solvent has a direct impact on the catalytic performance in oxidation reactions. In this work, we performed various experiments to know the influence of solvent by changing the solvents over the $Ce_{0.8}Zr_{0.2}O_2$ catalyst at 413 K and 20 bar O_2 pressure. Both polar and non-polar solvents were chosen to perform the reaction and the obtained results are presented in Fig. 6. It is apparent from the figure that the nature of solvent plays a remarkable role in the conversion of vanillyl alcohol. For instance, the use of toluene and hexane solvents yielded ~23 and ~30% conversion of vanillyl alcohol. These solvents are highly non-polar, which facilitate poor solubility of vanillyl alcohol in the reaction mixture leading to poor interaction with the catalyst and resulted in low activity. In contrast, we have achieved ~52% conversion in ethyl acetate solvent, which is due to high solubility of vanillyl alcohol facilitated by the polar nature of ethyl acetate. The catalytic efficiency of vanillyl alcohol was further improved with the increase of polarity of solvents. We achieved ~65, 80 and ~98% vanillyl alcohol conversion for isopropanol, 1,4-dioxane and acetonitrile solvents, respectively. The high conversion of vanillyl alcohol (~98%) and superior selectivity (~99%) to vanillin in acetonitrile solvent is attributed to its high polarity. The

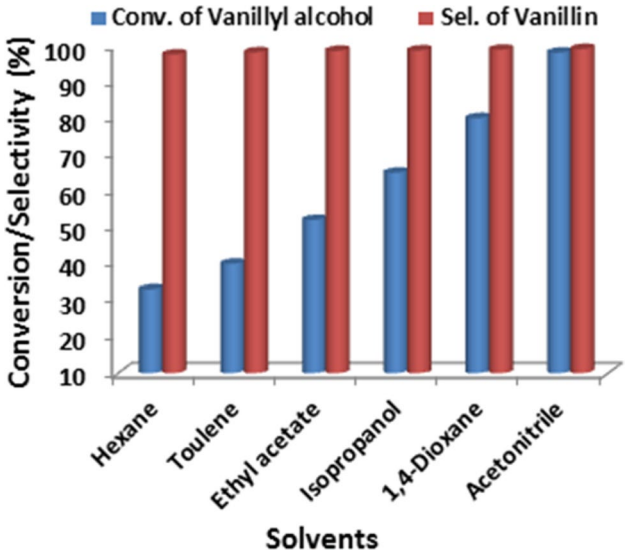

Fig. 6 Effect of solvent on selective oxidation of vanillyl alcohol over $Ce_{0.8}Zr_{0.2}O$ catalyst. Reaction conditions: vanillyl alcohol (3 mmol), time (5 h), temperature (413 K), catalyst (150 mg), O_2 pressure (20 bar), and acetonitrile (20 ml)

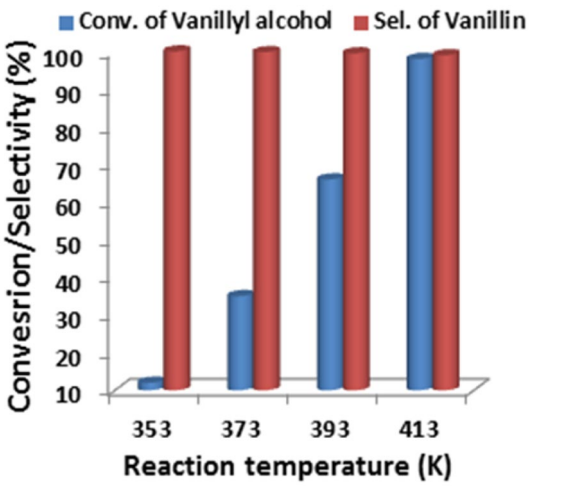

Fig. 7 Effect of reaction temperature on selective oxidation of vanillyl alcohol over $Ce_{0.8}Zr_{0.2}O_2$ catalyst. Reaction conditions: vanillyl alcohol (3 mmol), time (5 h), catalyst (150 mg), O_2 pressure (20 bar), and acetonitrile (20 ml)

polarity of various solvents are in the following order: acetonitrile > 1,4-dioxane > isopropanol. Striking observation noted in this study is that irrespective of the nature of solvent all showed high selectivity to vanillin. Therefore, we have chosen acetonitrile as the solvent to optimize other reaction parameters.

3.9 Effect of Reaction Temperature

Reaction temperature is one of the key factors, which effectively influences the rate of reaction in terms of conversion and selectivity of products. Therefore, the role of reaction temperature was studied for the oxidation of vanillyl alcohol by varying the temperature from 353 to 413 K using acetonitrile as the solvent at 20 bar O_2 pressure over the high efficient $Ce_{0.8}Zr_{0.2}O_2$ catalyst. The obtained results are illustrated in Fig. 7. It is obvious from the figure that a low conversion of vanillyl alcohol (~12%) was noticed at 353 K, which is due to the availability of less number of vanillyl alcohol molecules to react with the active sites during the catalytic reaction. Interestingly, we observed a ~100% selectivity to vanillin indicating that our catalytic system is highly selective even at low reaction temperatures. While increase in the reaction temperature from 353 to 373 K, a notable improvement i.e., ~12 to ~35% in the conversion of vanillyl alcohol was observed. When we increased the reaction temperature to 393 K, the conversion of vanillyl alcohol markedly improved to ~66%. Further increase in the temperature to 413 K, a high conversion of vanillyl alcohol (~98%) with ~99% selectivity to vanillin was noticed. Irrespective of the temperature used, a high selectivity to vanillin was found. Thus, it is concluded that 413 K is the optimized reaction temperature for oxidation of vanillyl alcohol.

3.10 Effect of Reaction Time

The influence of reaction time on vanillyl alcohol oxidation was studied by varying the time from 1 to 5 h using acetonitrile solvent over $Ce_{0.8}Zr_{0.2}O_2$ catalyst at 413 K and 20 bar O_2 pressure. The achieved results are illustrated in Fig. 8. As expected, the conversion of vanillyl alcohol markedly increased with increase of reaction time. It is noteworthy that a high conversion of vanillyl alcohol (~46%) with high selectivity to vanillin (~99%) was achieved with 1 h time, which signifies that our developed $Ce_{0.8}Zr_{0.2}O_2$ catalyst is efficient and selective even at short reaction times. The conversion of vanillyl alcohol was found to increase from ~46 to ~98% as the time increases from 1 to 5 h without affecting the selectivity to vanillin product. The achieved vanillyl alcohol conversions are ~46, ~62, ~84, ~90, and ~98% for 1, 2, 3, 4 and 5 h of reaction times, respectively. Thus, 5 h is the optimized reaction time to obtain high catalytic efficiency for oxidation of vanillyl alcohol.

3.11 Effect of O_2 Pressure

The role of oxygen pressure was also examined for selective oxidation of vanillyl alcohol in the range of 5–20 bar O_2

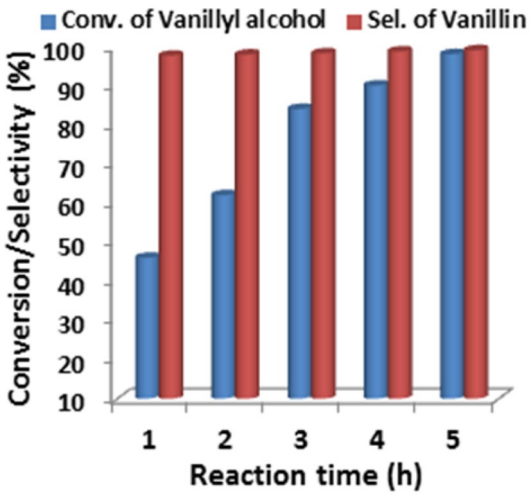

Fig. 8 Effect of reaction time on selective oxidation of vanillyl alcohol over $Ce_{0.8}Zr_{0.2}O_2$ catalyst. Reaction conditions: vanillyl alcohol (3 mmol), temperature (413 K), catalyst (150 mg), O_2 pressure (20 bar), and acetonitrile (20 ml)

pressure (reaction conditions: 3 mmol of vanillyl alcohol, 150 mg of catalyst, 20 ml of acetonitrile, 413 K, 5 h, and $Ce_{0.8}Zr_{0.2}O_2$ catalyst) (Fig. 9). It is clearly observed that the O_2 pressure showed a significant impact on the catalytic efficiency. It is obvious from the Fig. 9 that, ~74% conversion and ~99% selectivity to vanillin was obtained at 5 bar oxygen pressure indicating that our newly designed catalyst is highly active for selective for oxidation of vanillyl alcohol at low O_2 pressure. As the pressure increased from 5 to 10 bar, the conversion of vanillyl alcohol was increased from ~74 to ~85% and no change in the selectivity to vanillin was noted. Further increase in the pressure to 20 bar, an increase in the catalytic activity (~98%) was observed, which is due to the availability of high amount oxygen to participate in the oxidation reaction. Hence, based on the catalytic results a 20 bar O_2 pressure was identified as the optimum to achieve better catalytic results for this reaction.

3.12 Recyclability Studies

Recyclability of the catalyst is one of the key factors in heterogeneous catalysis. Therefore, we have studied the recyclability of high efficient $Ce_{0.8}Zr_{0.2}O_2$ catalyst to understand its stability towards oxidation of vanillyl alcohol. The reaction conditions fixed were as follows: vanillyl alcohol (6 mmol), catalyst amount (300 mg), O_2 pressure (20 bar), reaction time (5 h), acetonitrile solvent (40 ml), and 413 K temperature. After completion of each cycle, the catalyst was subjected to separation and washed thoroughly with deionized water followed by methanol for several times and finally dried at 393 K for 6 h. Under identical conditions, we continued this process up to five cycles and the obtained results are depicted in Fig. 10. As can be noticed from the Fig. 10, there is insignificant variation in the conversion of vanillyl alcohol up to five cycles. However, there is a continuous slight drop in the conversion indicating a slight deactivation of the catalyst, which is ascribed to the unfavorable physicochemical properties of the recycled catalysts. Further studies are necessary to understand this fact which is under active investigation. The conversion of vanillyl alcohol in the 1st, 2nd, 3rd, 4th and 5th cycle were ~98, ~95, ~93, ~90 and ~89%, respectively. Irrespective of the catalytic cycle, no appreciable change in the selectivity to vanillin was noticed.

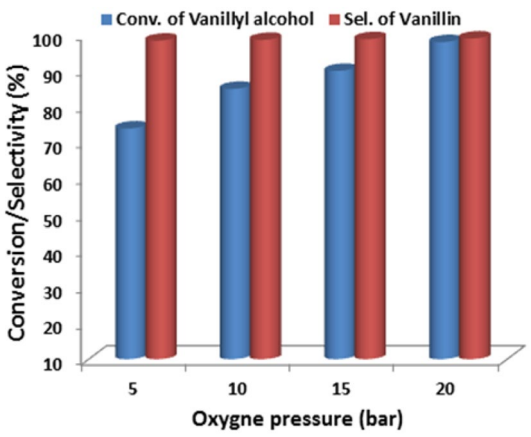

Fig. 9 Effect of O_2 pressure on selective oxidation of vanillyl alcohol over $Ce_{0.8}Zr_{0.2}O_2$ catalyst. Reaction conditions: vanillyl alcohol (3 mmol), temperature (413 K), time (5 h), catalyst (150 mg), and acetonitrile (20 ml)

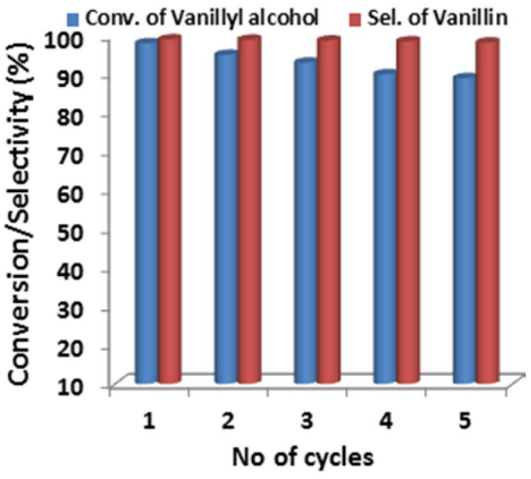

Fig. 10 Recyclability of $Ce_{0.8}Zr_{0.2}O_2$ catalyst for selective oxidation of vanillyl alcohol. Reaction conditions: vanillyl alcohol (6 mmol), temperature (413 K), time (5 h), catalyst (300 mg), and acetonitrile (40 ml)

3.13 Comparative Study with Reported Catalysts

Finally, we have carried out a comparative study in the catalytic performance and selectivity to vanillin over our developed Ce–Zr–O mixed oxide catalyst with the recently reported catalysts for oxidation of vanillyl alcohol and the data is presented in Table S1. Various metal oxides and mixed metal oxide catalysts were studied for the oxidation of vanillyl alcohol. For instance, $CuZrO_3$ catalyst exhibited ~ 91% conversion, but shows moderate selectivity to vanillin (~ 76%) [16]. On the other hand, Co_3O_4 shows ~ 80% conversion with high selectivity to vanillin (98%), whereas MnCo–MO catalyst provided moderate conversion (~ 62%) of vanillyl alcohol with ~ 83% selectivity to vanillin product [6, 7]. Further, ~ 89 and 91% conversions were achieved with Mn-doped CeO_2 and Cu–Mn mixed oxides [8, 18] respectively. Compared to the reported catalysts, our developed $Ce_{0.8}Zr_{0.2}O_2$ catalyst shows a high activity in terms of conversion and product selectivity indicating that the present catalyst is promising for the selective oxidation vanillyl alcohol.

3.14 Structure–activity Relationship

Based on the characterization studies and activity results, some critical properties such as BET surface area, oxygen vacancies, and high redox ability could be identified as the decisive factors for $Ce_{0.8}Zr_{0.2}O_2$ nanocatalyst to achieve an excellent catalytic performance in the vanillyl alcohol oxidation. For instance, surface area of the catalyst is one of the influencing factors in vanillyl alcohol oxidation. High surface area accompanying catalyst not only beneficial to yield highly dispersed active sites but also improves the contact area between the active species and vanillyl alcohol leading to excellent activity. The developed $Ce_{0.8}Zr_{0.2}O_2$ catalyst exhibited a high BET surface area (~ 137.1 m^2/g) (Table 1) compared to other investigated catalysts. Several studies demonstrated that oxygen vacancies play a key role in promoting the oxidation reactions particularly, adsorption and activation of gaseous phase oxygen facilitated by oxygen vacancies in order to interact with the reactant molecules. From Raman studies (Fig. 2), the $Ce_{0.8}Zr_{0.2}O_2$ catalyst showed a high concentration of oxygen vacancies, thereby exhibited superior catalytic activity in the oxidation of vanillyl alcohol.

In addition, redox properties show significant impact on the vanillyl alcohol oxidation. Since, high redox ability could facilitate to yield more active oxygen species, which significantly promote the vanillyl alcohol oxidation. It can be noted from Fig. 5 that rich Ce content $Ce_{0.8}Zr_{0.2}O_2$ nanocatalyst exhibited a high redox nature hence superior catalytic performance. The novelty of present work could be pointed out by several factors. Most of the catalysts reported for oxidation of vanillyl alcohol adversely affected by the use of organic peroxides and bases, which usually generate large amounts of toxic chemical wastes and require a tedious workup procedure for separating the catalysts from the reaction mixtures as well as for analysing the reaction products. In the present work, the catalytic experiments were performed using molecular oxygen as sole oxidant under base-free conditions, which is greener and can be considered as more efficient methodology.

4 Conclusions

In this study, the influence of Ce/Zr mole ratio on the physicochemical properties and their catalytic activity was evaluated for Ce-Zr-O mixed oxides. Accordingly, Ce_{1-x}-$Zr_xO_{2-\delta}$ (x = 0.2, 0.5, and 0.8) solid solutions were synthesized by adopting a facile coprecipitation method and investigated for aerobic oxidation of vanillyl alcohol under base-free conditions. Based on the physicochemical properties, it was found that $Ce_{0.5}Zr_{0.5}O_2$ and $Ce_{0.8}Zr_{0.2}O_2$ catalysts had a cubic CeO_2 phase, while tetragonal ZrO_2 phase was noticed for $Ce_{0.2}Zr_{0.8}O_2$ sample (XRD results). High concentration of oxygen vacancies was observed for $Ce_{0.8}Zr_{0.2}O_2$ sample (Raman studies). TPR studies revealed a high redox nature for Ce rich Ce–Zr oxides namely, $Ce_{0.5}Zr_{0.5}O_2$ and $Ce_{0.8}Zr_{0.2}O_2$, which profoundly influenced the catalytic activity for vanillyl alcohol oxidation. The catalytic performance of Ce–Zr–O solid solutions with different Ce/Zr mole ratios was as follows: $Ce_{0.8}Zr_{0.2}O_2$ (~ 98%) > $Ce_{0.5}Zr_{0.5}O_2$ (~ 75%) > $Ce_{0.2}Zr_{0.8}O_2$ (~ 58%). Larger BET surface area, smaller crystallite size, strong synergetic interaction, improved oxygen vacancies, and a high redox nature together play a crucial role in obtaining the superior catalytic results for $Ce_{0.8}Zr_{0.2}O_2$ catalyst in the oxidation of vanillyl alcohol. Further, optimization of reaction parameters was established and also recyclability studies were performed on the high efficient $Ce_{0.8}Zr_{0.2}O_2$ catalyst up to 5 cycles without a significant loss of activity and selectivity.

Acknowledgements PRGNR and BG thank the Council of Scientific and Industrial Research (CSIR), New Delhi for the research fellowships. BMR thanks the Department of Atomic Energy (DAE), Mumbai for the award of Raja Ramanna Fellowship.

Compliance with Ethical Standards

Conflict of interest The authors declare no conflict of interest.

References

1. Rinesch T, Mottweiler J, Puche M, Concepción P, Corma A, Bolm C (2017) ACS Sustain Chem Eng 5:9818

2. Sudarsanam P, Zhong R, Bosch SV, Coman SM, Parvulescu VI, Sels BF (2018) Chem Soc Rev 47:8349
3. Deng W, Zhang H, Wu X, Li R, Zhang Q, Wang Y (2015) Green Chem 17:5009
4. Baguc IB, Celebi M, Karakas K, Ertas IE, Keles MN, Kaya M, Zahmakiran M (2017) Chem Select 2:10191
5. Fu W, Yue L, Duan X, Li J, Lu G (2016) Green Chem 18:6136
6. Jha A, Rode CV (2013) New J Chem 37:2669
7. Jha A, Rode CV, Patil KR (2013) Chem Plus Chem 78:1384
8. Ramana S, Govinda Rao B, Venkataswamy P, Rangaswamy A, Reddy BM (2016) J Mol Catal A Chem 415:113
9. Behling R, Valange S, Chatel G (2016) Green Chem 18:1839
10. Behera GC, Parida K (2012) Appl Catal A413:245
11. Ma R, Xu Y, Zhang X (2015) Chem Sus Chem 8:24
12. Wu X, Guo S, Zhang J (2015) Chem Commun 51:6318
13. Rodriguez MM, Saravanamurugan S, Kegnæs S, Riisager A (2015) Top Catal 58:1036
14. Govinda Rao B, Sudarsanam P, Rangaswamy A, Reddy BM (2015) Catal Lett 145:1436
15. Jha A, Mhamane D, Suryawanshi AB, Joshi SM, Shaikh P, Biradar NS, Ogale S, Rode CV (2014) Catal Sci Technol 4:1771
16. Saha S, Hamid SBA (2017) RSC Adv 7:9914
17. Yuan Z, Chen S, Liu B (2017) J Mater Sci 52:164
18. Saha S, Hamid SBA (2016) RSC Adv 6:96314
19. Saha S, Hamid SBA, Ali TH (2017) Appl Surf Sci 394:205
20. Govinda Rao B, Sudarsanam P, Nallappareddy PRG, Reddy MY, Rao TV, Reddy BM (2017) Catal Commun 101:57
21. Wang WW, Yu WZ, Du PP, Xu H, Jin Z, Si R, Ma C, Shi S, Jia CJ, Yan CH (2017) ACS Catal 7:1313
22. Govinda Rao B, Jampaiah D, Venkataswamy P, Reddy BM (2016) Chem Select 1:6681
23. Rodriguez JA, Grinter DC, Liu Z, Palomino RM, Senanayake SD (2017) Chem Soc Rev 46:1824
24. Shang D, Cai W, Zhao W, Bu Y, Zhong Q (2014) Catal Lett 144:538–544
25. Mukherjee D, Govinda Rao B, Reddy BM (2016) Appl Catal B Environ 197:105
26. Cao D, Cai W, Li Y, Li C, Yu H, Zhang S, Qu F (2017) Catal Lett 147:2929
27. Liu B, Li C, Zhang G, Yao X, Chuang SSC, Li Z (2018) ACS Catal 8:10446
28. Devaiah D, Reddy LH, Park SE, Reddy BM (2018) Cat Rev Sci Eng 60:177
29. Bonk A, Remhof A, Maier AC, Trottmann M, Schlupp MVF, Battaglia C, Vogt UF (2016) J Phys Chem C 120:118
30. Devaiah D, Tsuzuki T, Aniz CU, Reddy BM (2015) Catal Lett 145:1206
31. Li J, Liu X, Zhan W, Guo Y, Guo Y, Lu G (2016) Catal Sci Technol 6:897
32. Wang SP, Zhang TY, Su Y, Wang SR, Zhang SM, Zhu BL, Wu SH (2008) Catal Lett 121:71
33. Govinda Rao B, Sudarsanam P, Nallappareddy PRG, Reddy MY, Rao TV, Reddy BM (2018) Res Chem Intermed 44:6151
34. Katta L, Sudarsanam P, Thrimurthulu G, Reddy BM (2010) Appl Catal B 101:101
35. Singhania A, Gupta SM (2018) Catal Lett 148:2001
36. Sudarsanam P, Hillary B, Mallesham B, Rao BG, Amin MH, Nafady A, Alsalme AM, Reddy BM, Bhargava SK (2016) Langmuir 32:2208
37. Govinda Rao B, Sudarsanam P, Mallesham B, Reddy BM (2016) RSC Adv 6:95252
38. Sudarsanam P, Hillary B, Deepa DK, Amin MH, Mallesham B, Reddy BM, Bhargava SK (2015) Catal Sci Technol 5:3496
39. Gong X, Liu B, Kang B, Xu G, Wang Q, Jia C, Zhang J (2017) Mol Catal 436:90
40. Lin X, Zhao S, Fu L, Luo Y, Zhu R, Liu Z (2017) Mol Catal 437:18
41. Xie Q, Zhao Y, Guo H, Lu A, Zhang X, Wang L, Chen MS, Peng DL (2014) ACS Appl Mater Interfaces 6:421
42. Zhang H, Gu F, Liu Q, Gao J, Jia L, Zhu T, Chen Y, Zhong Z, Su F (2014) RSC Adv 4:14879
43. Liwei J, Meiqing S, Jun W, Xia C, Jiaming W, Zhichang H (2008) J Rare Earths 6:523
44. Mandala S, Santra C, Bando KK, James OO, Maityc S, Mehtad D, Chowdhury B (2013) J Mol Catal A 378:47
45. Pengpanich S, Meeyoo V, Rirksomboon T, Bunyakiat K (2002) Appl Catal A 234:221